Dentomaxillofacial Radiology (2019) 48, 20180075

birpublications.org/dmfr

RESEARCH ARTICLE

Comparison of segmented thermal images versus a CT scanning for detection of maxillofacial pathology

[1]Diana Macianskyte, [1]Egle Monastyreckiene, [1]Algidas Basevicius and [2]Rimas Adaskevicius

[1]The Clinic of Radiology, Lithuanian University of Health Sciences, Kaunas, Lithuania; [2]Department of Electrical Power Systems, Kaunas University of Technology, Kaunas, Lithuania

Objectives: To evaluate thermal images (TIs) by using an algorithm for optimized region of interest (ROI) and image segmentation, in order to find zones of the facial skin surface with asymmetrical temperature, and to test consistency with CT findings, to detect maxillofacial pathologies (*i.e.* tumours).
Methods: The following steps for the TI evaluation were applied: data acquisition/pre-processing of frontal face and mouth projection, detection of face and mouth external contour, finding face and mouth symmetry axis, calculation of differences in average and maximal temperatures between left and right face and mouth sides, image segmentation of the selected ROI, and evaluation of diagnostic accuracy by comparing the TI results with CT findings.
Results: In healthy subjects, the average temperature difference between left/right sides of facial and mouth ROI was negligible (0.02 ± 0.21 °C and 0.05 ± 0.19 °C, respectively; $n = 23$). In the presence of tumour, the average temperature difference was higher in corresponding TIs (0.47 ± 0.1 °C and 0.66 ± 0.1 °C, for facial and mouth ROI, respectively; $n = 19$, $p < 0.05$). For large tumours, thermal asymmetry in the corresponding TI is easily detected, and image segmentation is optional for finding the affected zone. For small or deeply localized tumours, segmentation of the mouth cavity of the ROI was required for the detection of hot and cold spots.
Conclusions: Asymmetrical temperature zones and their location as detected from thermal images coincide well with the presence and localization of maxillofacial pathologies (*i.e.* tumours) established by CT. However, accurate information could often be obtained only after application of image segmentation algorithm to the selected ROI.
Dentomaxillofacial Radiology (2019) **48**, 20180075. doi: 10.1259/dmfr.20180075

Cite this article as: Macianskyte D, Monastyreckiene E, Basevicius A, Adaskevicius R. Comparison of segmented thermal images versus a CT scanning for detection of maxillofacial pathology. *Dentomaxillofac Radiol* 2019; **48**: 20180075.

Keywords: Infrared; thermal imaging; CT; segmentation algorithm; maxillofacial pathology

Introduction

Infrared thermography (IRT) is a non-invasive, non-contact as well as inexpensive diagnostic method. Because of its possibly high availability to large populations, its meets the essential requirements for a screening modality for pathology (*e.g.* tumour) detection.[1,2] Nevertheless, it is still not used for routine clinical diagnosis, largely because the desired information cannot be easily extracted.

The first attempt to measure human facial temperature has been made as early as in 1996.[3] However, possibilities to use IRT for detecting the presence of local lesions in the orofacial region in humans have been poorly explored, because the analysis of thermal images (TIs) in the maxillofacial part is complicated due to its elaborate anatomical structure. Therefore, for reliable IRT analysis it is important to use the computational algorithms. Development and application of adequate

Correspondence to: Mrs Diana Macianskyte, E-mail: diana.macianskyte@lsmuni.lt

Received 21 February 2018; revised 18 January 2019; accepted 25 January 2019

algorithms might help detect changed skin temperature distribution in the affected zones, and automatically processed evaluation of the images could possibly avoid overdiagnosis when interpreting TI data. It has been shown that accurate detection of the TI of the region of interest (ROI) and use of image segmentation are critical steps in the analysis,[4] to help revealing lesions more precisely.

In this study, we applied a new algorithm and demonstrate that image segmentation of optimized ROI allow detection of asymmetrical changes of skin temperature in the maxillofacial region. We also aimed to examine any relationship between the IRT and CT results, when comparing the asymmetrical temperature zones and their location in the TI with the lesions revealed during CT.

Methods and materials

The study was carried out in accordance with the European Community guiding principles outlined in the Declaration of Helsinki, and was approved by the Ethics Committee of Biomedical Research of Kaunas Region, Lithuania (No.BE-2-31). We investigated 42 human subjects (23 males and 19 females) with an age range of 15–86 years. They included patients (n = 19) who after clinical evaluation were directed to a CT procedure (in 2016) for suspected diagnosis of tumour in the orofacial/maxillofacial region [16 males and 3 females; mean (± standard deviation) age of 61.1 ± 4.5 and 71.0 ± 11.0 years, respectively] and healthy volunteers (n = 23; 7 males and 16 females; mean age 40.4 ± 6.0 and 51.3 ± 4.0 years, respectively), who were directed for CT evaluation before the planning of tooth implantation. The inclusion criteria was that the subject underwent a CT procedure for a first time, and had no prior surgical or drug treatment in the maxillofacial region. The exclusion criteria were a history of surgical procedures and/or traumatic injuries in maxillofacial region, a drug treatment, or the presence of other, non-cancerous pathologies. The procedures were explained to each of the subjects, and written informed consent was obtained.

Data acquisition

Because there are various factors which might affect the TI data, all patients were asked to avoid using medications, massage, physical exercise, facial cosmetics, shaving, smoking, alcohol drinking, intake of tea or coffee and large meals at least 1 h prior to the start of IRT measurements.[5]

At a first step, prior to the CT scanning procedure, the standardized thermograms were recorded for everyone subject. This was done in order to avoid the subsequent influence of X-rays and contrast agent on the temperature profiles of the face. All subjects underwent the same thermographic protocol adjusted for clinical application. Before starting IRT measurements, all patients were thermo-equilibrated for 15 min in the laboratory space (*i.e.* with a constant temperature, humidity, no direct sunlight etc.).[6] During the measurements each patient was instructed to sit up straight, and the head was positioned in front of an infrared thermal camera. Under the conditions of this study, the camera was placed 1 m from the patient's face. The camera's lens was manipulated to bring the subject's face into focus. The TIs of the face were taken in both the frontal closed and open mouth projections. The TIs were coded and stored on computer, to be later analyzed by an experienced thermographer.

At the next step, each patient was scanned with a multislice CT (Toshiba *Aquilion ONE*, Canon Medical Systems, Japan), using identical scanning parameters (contiguous 1 mm thick axial slices). All CT images were analyzed by an experienced radiologist, and the diagnosis of the maxillofacial pathology was determined.

Finally, based on CT findings the diagnostic accuracy of a new algorithm for TI analysis was evaluated. To be able of comparing these data, the special procedures were followed: pre-processing of the TI, detection of the face/mouth edges, finding of the face/mouth symmetry axis, calculation of temperatures (averaged and peak) of the ROI, and image segmentation of the selected ROI. The schematic experimental set-up and the sequence of algorithmic calculations is presented in Figure 1.

Face contour detection

The pre-processing of TIs starts with checking the thermal data structure (Table 1): the environment conditions, the distance to camera, the emissivity of the body etc. Then the edges of human face were determined (Figure 1b). The proper detection of facial edge in a TI is an important process which allows preserving its important structural characteristics, while reducing the unwanted data from an image. In order to extract such information, the image gradients created from the original TI were used by looking for the maximum and minimum in the first derivative of the temperature. Hence, each pixel of a gradient image (∇f) measures the change in temperature (∂I) of that same point in the original image in a given direction. To get the full range of direction, the gradient images in the x and y directions were computed as first order derivatives of thermal image I in x and y direction:

$$\nabla f_x = \frac{\partial I}{\partial x}, \qquad \nabla f_y = \frac{\partial I}{\partial y}. \tag{1}$$

At each point in the image, the resulting gradient magnitude was calculated using[7]:

$$\nabla f = \sqrt{\nabla f_x^2 + \nabla f_y^2}. \tag{2}$$

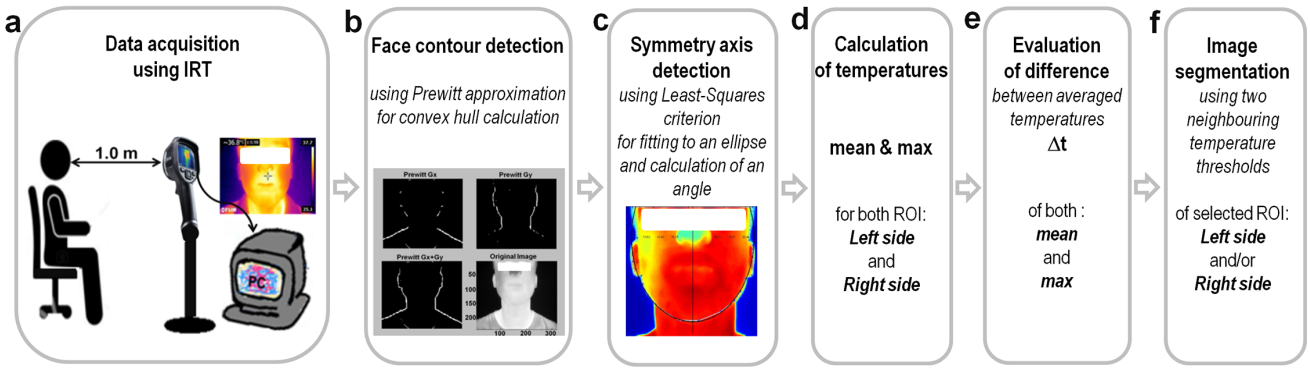

Figure 1 Schematic experimental system and principal steps of usage an algorithm for the analysis of thermal images. An infrared camera was mounted on an upright frame and located 1.0 m from the face of the subject to be examined (a). The following main steps for TI evaluation were applied: (a) acquisition/pre-processing and storage of raw thermal data, (b) detection of human face edges by creating image gradients (G_x and G_y- the convolution mask along x-axis and y-axis, respectively), (c) finding of orientation and position of the symmetry axis (Note: the larger axis of an ellipse matches with the symmetry axis of the human face), (d) calculation of average and peak temperatures of both left/right facial ROI, (e) evaluation of temperature differences (averaged and peak), and (f) image segmentation (if necessary) of selected facial ROI. The same steps were used for analysis of the mouth cavity ROI. IRT, infrared thermography; ROI, region of interest; TI, thermal image.

A Prewitt approximation was used, due to its simplicity and low computational load, to find edges at points[8] where the gradient values are maximal. An original human face contour detection is presented in Figure 1b. For the presentation of human face external contour as the smallest convex polygon that contains all points of the edge, the convex hull was calculated using the Quick Hull method.[9] This convex hull was used to describe the external boundary of the field in which temperature changes were analyzed.

Finding the position and orientation of the symmetry axis

Asymmetrical temperature distribution is an indicator of lesion (*i.e.* pathology).[10] Finding of facial symmetry axis allows to separate left and right sides of the face and to calculate skin temperature difference (Δt) between both sides by subtracting the right side-value from the left.

The best fitting of human face edges to an ellipse, formed from set of convex hull vertices, was used for the identification of the facial axis symmetry (Figure 1c). The least-squares criterion was used for the best fit estimation. Hence, the major semi-axis of the ellipse represents the facial symmetry axis, which was used for splitting the field of analysis into two independent (left and right side) areas. Then, the average (Δt_{mean}) and the maximal (Δt_{max}) temperatures were calculated and compared for both sides of the human face (Figure 1d–e). Temperature asymmetry higher than 0.4 °C was taken as indication of the presence of a pathology.[11] The mouth cavity was investigated using a similar approach and temperature asymmetry evaluated.

Image segmentation of the left/right region of interest

The appropriate side-of the ROI image was used for determining isolines along which the temperature has a constant value. The thresholding method for image segmentation (Figure 1f) was used. This method is based on threshold value to turn the region of TI into a binary image. Using two neighbouring temperature thresholds $t_i + \Delta t/2$ and $t_i - \Delta t/2$, a range of temperatures related to the region:

$$t_i + \Delta t/2 > t_i > t_i - \Delta t/2 \tag{3}$$

can be defined as binary area $g(x, y)$ having t_i temperature. Δt is the temperature range of segment or temperature difference between neighbouring isolines. A filled contour plot for displaying isolines and filling the areas $g(x, y)$ between the isolines using constant colours, corresponding to the current temperature t_i colour map, can be defined as:

$$g(x, y)=\begin{cases} t_{i+1}, & \text{if } T(x, y) > t_i \\ t_i, & \text{if } t_i + \Delta t/2 > T(x, y) \geq t_i - \Delta t/2 \\ t_{i-1}, & \text{if } T(x, y) \leq t_i \end{cases}, \tag{4}$$

Table 1 Measurement conditions for the TI session

Input quantity	*Setting the emissivity as object surface property*	*Room temperature (°C)*	*Relative humidity (%)*	*Subject rest time before test (min)*	*Camera-to-object distance (m)*
Estimate values	0.98	22 ± 0.1	60 ± 5	15 ± 0.2	1

Of note: there was no direct sunlight in the room, and air conditioning was switched off during the measurements. Values measured with an infrared camera were stored in a computer file.

where $T(x, y)$ is the temperature of TI pixel at particular location x, y.

The colour map is a representative tool for the evaluation of facial pathology. The number and values of the isolines are chosen automatically based on the minimum and maximum values of face area. TIs were analyzed in respect of the skin and mouths mucosal lining (epithelium) temperature differences between the affected side and the opposite normal side. The pathological region has different temperature range and it can be highlighted in different colour from the rest of the face. The place and side of facial/mouth asymmetrical temperature identified in the TI was compared with the findings of CT.

Evaluation of diagnostic accuracy

Patients with suspected diagnosis of maxillofacial tumour were involved in this study. In general, CT was used detect the presence of a tumour in the orofacial/maxillofacial region. As mentioned above, the CT images were analyzed by a radiologist. The CT-generated information on the absence/presence of lesion and of its location was compared with the TI results for the same patient (*i.e.* we checked whether the appearance of asymmetrical temperature zone in the TI of selected ROI as well as its location coincided with a CT data).

IRT imaging equipment

TIs were acquired using a commercially available infrared thermal camera *FLIR E8* (*FLIR Systems, Inc.,* USA). The camera's thermal sensitivity is 0.06 °C, resolution is 320 × 240 pixels, and maximum temperature range is −20 °C up to + 250 °C. All surface temperature profiles were analyzed using an image processing software developed in *Matlab R2014b* (*The MathWorks, Inc.,* USA). The images were transformed into *Matlab* readable data files by using special software *ThermaCam Researcher 2.1* (*FLIR Systems*, *Inc*., USA). It is to be noted that each TI must carry tinformation such as temperature range with colour temperature scale, emissivity of body, atmospheric temperature, relative humidity, and patient-to-camera distance (Table 1).

Data analysis and statistics

The maximal and average temperatures of four human face areas (two facial sides: left and right; and two mouth cavity sides: left and right) were computed five times in each image for normal and pathological cases. All measurements were expressed as *mean ± standard deviation (SD)*. The *t*-test was used to evaluate whether the means of left and right sides are statistically different from each other. The significance level was set at $p < 0.05$. The two-sample *t*-test analysis was performed in *Matlab*.

Results

Representative examples of TI maps from the frontal projection of human face (a) and of mouth cavity (b) of a healthy subject (Case 1) are shown in Figure 2. The TIs were processed in two steps, through the algorithmic procedures for detecting the external contour of the ROI and finding position of the symmetry axis. Calculated temperatures for left/right sides of the selected ROI are presented in Table 2 (see Case 1). Importantly, in all healthy subjects (n = 23) there was no evident thermal asymmetry in the TIs of the four areas examined: 35.85 ± 1.31 °C *vs* 35.82 ± 1.33 °C for left and right side of the face, respectively, and 36.72 ± 1.55 °C *vs* 36.77 ± 1.58 °C for left and right side of the mouth cavity. In these subjects, calculated Δt_{mean} (difference in mean temperature) between the left/right sides of both facial and mouth ROIs was negligible (0.02 ± 0.21 °C and 0.05 ± 0.19 °C, respectively). In addition, Δt_{max} (difference in maximum temperature) values also were not significant (0.02 ± 0.19°C and 0.03 ± 0.25 °C, respectively; $p > 0.05$). It should be noted that these patients underwent a CT to evaluate the mandibular canal position before the planning of tooth implantation.

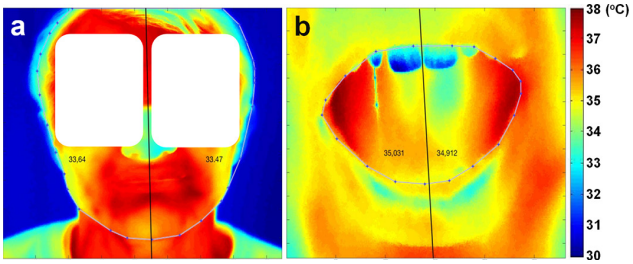

Figure 2 Thermographic images of young a 24-year-old male without any health problems. No lesion detected during a CT evaluation (not shown). Symmetrical temperature distribution of thermal images obtained in a healthy subject: in the frontal closed (a) and open-mouth projections (b) after finding the external contour of the ROI (*dot-dashed curve*) and the symmetry axis (*vertical line*). Note: no evident temperature changes in left/right sides. The corresponding scale bar is given on the right side of the image in °C. ROI, region of interest.

In contrast, in case of pathology such as benign (n = 4) or malignant (n = 15) tumour, as detected by CT, the TI of the same patients displayed a higher temperature difference profile. Representative cases are presented below.

Figure 3 shows a case of maxillofacial tumour. After clinical examination, the patient was directed to a CT procedure, because of visible deformity on the left side of the face. As illustrated in Figure 3a, an axial section of the CT scan image showed evident expansion on the left side of the mandible, with apparent ground-glass opacities and intact overlying bone and soft tissue. This patient had histologically proven benign tumour, namely fibrous dysplasia of the mandible. TI evaluation revealed thermal asymmetry at the corresponding facial side where lesion was present (Figure 3b), and the Δt_{mean} was of 0.87 °C. In addition, obvious thermal asymmetry was seen in the TI of mouth cavity, as presented in Figure 3c, where the pathological area is highlighted as higher colour intensity. The highest temperature in that area was > 38 °C (see Case 2 in Table 2). Of note, in this

Table 2 Calculated temperatures for left/right sides of the ROIs from the TIs presented in Figures 2–5

Presented Cases	*ROI*	t_{meanL} *(°C)*	t_{maxL} *(°C)*	t_{meanR} *(°C)*	t_{maxR} *(°C)*	Δt_{mean} *(°C)*	Δt_{max} *(°C)*	*IRT (0/1)*	*CT view*
Case 1, a healthy subject	f	33,93 ±0,039	36,17	33,77 ±0,04	36,03	0,16	0,14	0	No lesion detected
	m	35,08 ±0,013	36,97	34,92 ±0,023	36,78	0,16	0,19	0	
Case 2, the patient with benign tumour	f	34,42 ±0,019	36,45	33,55 ±0,017	36,23	0,87	0,22	1	Evident bone lesion on the left side-of the mandible
	m	37,84 ±0,023	38,97	37,29 ±0,217	38,33	0,55	0,64	1	
Case 3, the patient with malignant soft tissue tumour	f	35,50 ±0,054	38,14	35,52 ±0,032	37,96	0,28	0,18	1	A wide bone destruction zone on the right side-of the mandible
	m	36,85 ±0,01	38,15	36,91 ±0,017	38,57	−0,06	−0,42	1	
Case 4, the patient with malignant tumour (deeply located)	f	32,83 ±0,015	35,01	32,94 ±0,01	36,12	−0,11	−1,11	1	A hard palate bone destruction zone
	m	35,84 ±0,085	37,82	35,88 ±0,062	37,88	−0,04	−0,06	1	

IRT, infrared thermography; ROI, region of interest; TI, thermal image; f, facial; m, mouth.
t_{meanL} and t_{meanR}: calculated values in mean temperatures for left (L) and right (R) sides of the ROIs; t_{maxL} and t_{maxR}: detected values in maximum temperatures for left/right sides of the ROIs; Δt_{mean} and Δt_{max}: calculated differences in mean temperatures and in maximum temperatures between the left/right sides of the ROIs; IRT(0/1): the computer-generated information on the absence (0) or presence (1) of temperatures asymmetry detected by IRT; CT (view) : the CT-generated diagnosis on the absence/presence of lesion and of its location; Detected values presented as *mean* ± *SD*.

case thermal asymmetry was visible without additional image segmentation. Nevertheless, after segmentation the pathological zone became even more segregated and visible (Figure 3d).

Figure 4 shows another case of tumour, where the patient, after clinical examination, was directed for a CT procedure, because of a painful buccal mucosa on the right side. In this case facial deformity was negligible but in an axial CT image, as presented in Figure 4a, a wide bone destruction zone on the right side of the mandible was seen. The patient had histologically proven malignant soft tissue tumour, namely squamous cell carcinoma (SCC). Despite the huge bone lesion in the mandible, in the corresponding TI of the same patient only slight Δt_{mean} and Δt_{max} between left/right sides of the mouth cavity were detected (Figure 4c): 0.06 and 0.42 °C, respectively (see Case 3 in Table 2). However, after application of image segmentation (Δt = 0.5 °C) for the ROI, a higher temperature zone became visible in the affected side. Figure 4d shows highlighting of the pathological area with more intensive colouring. The highest temperature spot reached 39.0 °C.

In some pathological cases, deformity due to maxillofacial pathology can be negligible or even not visible. Figure 5 shows a case in which the patient complained of a weak pain deep in the mouth cavity during clinical examination and, therefore, was directed for a CT procedure. There was just very slight deformity of the right oropharyngeal wall. The CT image of the patient, presented in Figure 5a, displayed soft tissue infiltration of the velum and the right parapharyngeal region, with spread and local destruction of hard palate. Histopathological diagnosis was SCC. In this case, there was no visible thermal asymmetry in the TI of closed-mouth (Figure 5b). The average temperature difference between both sides of the face was just 0.1 °C (see Case 4 in Table 2). Even in the open-mouth position there was no clear temperature difference between right and left sides.

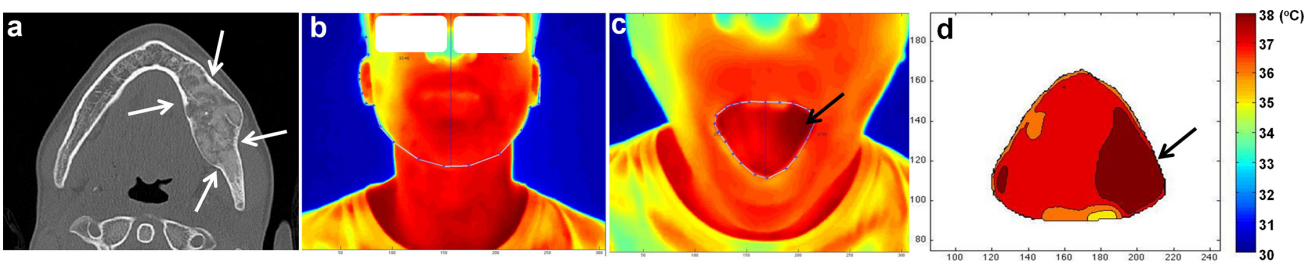

Figure 3 CT *vs* IRT images obtained in a 15-year-old male patient with fibrous dysplasia on the left side and with visible deformity of the mandible in axial CT image of affected jaw (a) *vs* TIs in frontal closed-mouth (b) and in open-mouth projections (c). Note: in CT image (a) expansion on the left side of the mandible with ground-glass opacities (marked by arrows) is evident. Accordingly, in the TIs there are evident asymmetrical temperature changes on the left side of the face (b) and of the mouth cavity before and after segmentation (c, d, respectively). Segmentation highlighted the lesion in dark (marked by arrow). Other notations are the same as in Figure 2. IRT, infrared thermography.

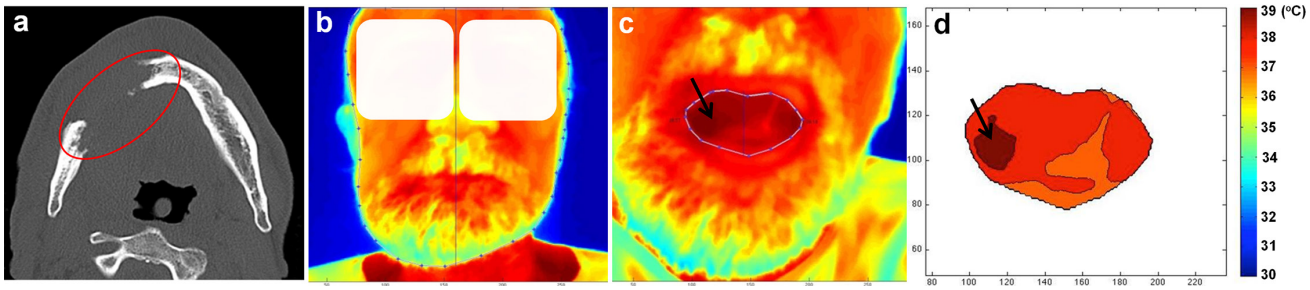

Figure 4 CT *vs* IRT images obtained in a 64-year-old male patient with obvious pathological changes of malignant soft tissue tumour (SCC) on the right side: in axial CT image of affected jaw (a) *vs* TIs in frontal closed-mouth (b) and in open-mouth projections (c). Note: in the CT image (a) of affected jaw there is a wide bone destruction zone of the body of the mandible on the right (marked by oval). In the TI of the mouth cavity, before and after segmentation (c, d, respectively), there is asymmetrical temperature on the right side, which the lesion region highlighted in dark (marked by arrow). Other notations are same as in Figure 2. IRT, infrared thermography; TI, thermal image; SCC, squamous cell carcinoma.

However, after application of the image segmentation algorithm (Δt = 1 °C) for the selected ROI, a local high temperature zone, positioned deeply in mouth cavity, appeared (Figure 5c).

A quantitative evaluation of all thermal images collected from patients with tumours (n = 19) showed higher temperature profiles in the affected region with respect to the surrounding normal tissues. Figure 6 illustrates histograms representing the distribution of the results of Δt_{max} and Δt_{mean}, calculated between left and right sides of the ROIs of human face and mouth, for both groups of all subjects of the current study. Of note, there was much wider distribution of temperature differences between left/right side of the selected ROIs in patients with maxillofacial tumours, when compared with the healthy subjects (Figure 6, e–h *vs* Figure 6 a–d) (see Discussion for possible reasons). In patients with tumour, the mean values obtained for the facial and mouth cavity ROIs were 0.47 ± 0.1 °C and 0.66 ± 0.1 °C, respectively, for the Δt_{mean} between left/right sides, and 0.33 ± 0.14 °C and 0.74 ± 0.18 °C, respectively, for the Δt_{max} between both sides. The differences between parameters for mouth cavity ROI obtained in patients with tumours were statistically significant in comparison with those obtained on healthy volunteers ($p < 0.05$).

Discussions

The overall aim of this study was to evaluate the use of improved TIs of the maxillofacial area in the diagnosis of tumours. Improved TIs were obtained using an image processing algorithm based on the optimized ROI and image segmentation, when searching of zones with asymmetrical temperature. We wanted to look for possible correspondence between IRT and CT results. The comparison revealed that the new algorithm, which automatically processes analysis of the thermal images, allows to detect lesions in the maxillofacial area and to clearly display its location in the left or right facial/mouth side, in consistence with CT evaluation for the same patient. However, in some cases, segmentation of the selected ROI was necessary for IRT for accurate detection of asymmetrical temperature.

Since diagnosis accuracy depends on how well the segmentation of the ROI was performed, we used an algorithm allowing to obtain optimized selected ROI. In our study, was calculated human facial/mouth external contour as smallest convex polygon that contains all points of the edge for both facial/mouth ROIs (see Methods and materials). This allowed to get very precise contouring of the selected ROI and overcome

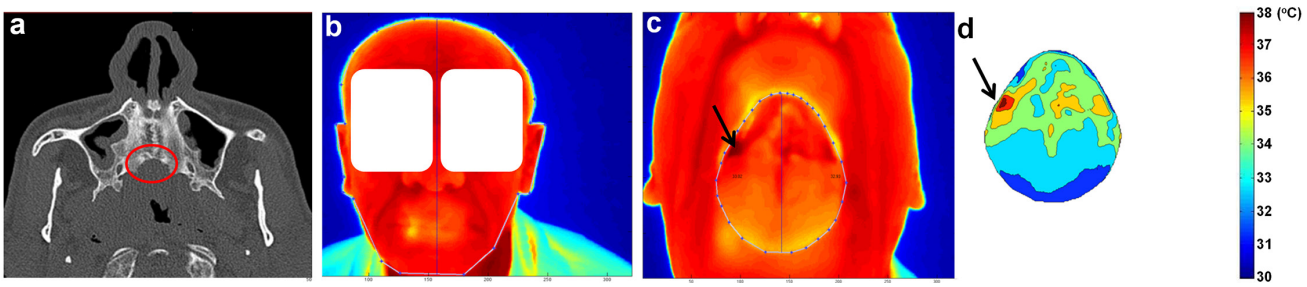

Figure 5 CT *vs* IRT images obtained in a 65-year-old male patient without visible facial deformity due to malignant tumour (SCC): on the axial CT image (a) *vs* frontal face TI (b) and open-mouth TIs before (c), and after segmentation (d), with the lesion region highlighted in dark colour (marked by arrow). Note: on the CT image (a) there is a hard palate bone destruction zone (marked by an ellipse). In the thermal image there is poor mouth's temperature asymmetry (c), but after segmentation (d) a clear zone with higher temperature is seen on the right side, with the lesion region highlighted in dark (marked by arrow). Other notations are same as in Figure 2. IRT, infrared thermography; TI, thermal image; SCC, squamous cell carcinoma.

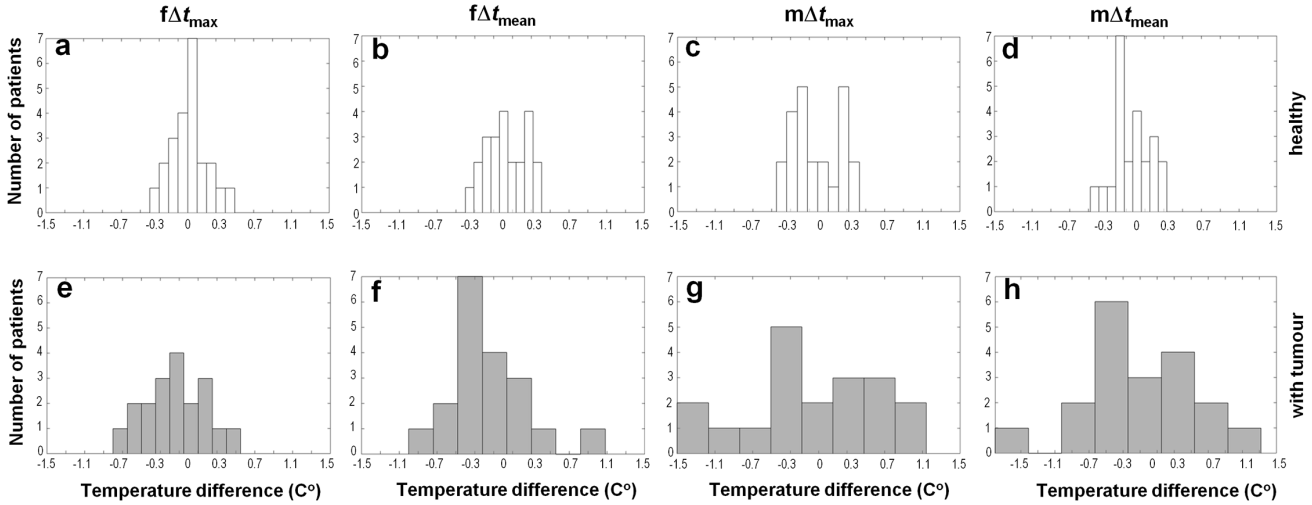

Figure 6 The distribution of temperature difference values for healthy subjects (a–d) *vs* patients with clinically confirmed maxillofacial tumours (e–h). fΔt_{mean} and fΔt_{max} : differences in mean temperatures (fΔt_{mean}) and in peak temperatures (fΔt_{max}) between left and right sides of the face. mΔt_{mean} and mΔt_{max}: differences in mean temperature (mΔt_{mean}) and in peak temperature (mΔt_{max}) between left and right side-of the mouth.

the inclusion of irrelevant data in evaluating of the TI, in contrast to previous studies,[12–14] in which geometric shapes were used to define the ROIs. In most applications, IRT images obtained using non-optimized software for the ROI detection contain information not only within the area to be characterized, but also from the surroundings. Consequently, this might not allow to detect modest asymmetry in TIs of small or deeply located lesion, especially when the lesion is close to the mandibular joint that only emits limited heat. Furthermore, small and/or modest asymmetry of the Δt may not be revealed due to eventual fat tissue, which is an effective insulator. Therefore, limited heat could be difficult to detect without algorithmic calculations. The algorithm used in the present study allows to overcome this limitation.

Besides, we tried to detect symmetrical/asymmetrical temperature distribution not in separate anatomical regions as was done in previous studies,[3,11] but between both (left/right) sides of the frontal face and mouth TIs. A critical step was the determination of a symmetry axis (see Methods and materials), which allowed to compare the Δt_{mean} and Δt_{max} values calculated from left versus the right sides of facial and mouth cavity images. When pathology was not detected upon CT evaluation, as in the case of the healthy subjects, then there was no temperature asymmetry between the sides of the selected ROI. In contrast, when CT delineated a tumour structure, later confirmed with histopathology (in most cases SCC), then the left-*vs*-right asymmetry in temperature was also obtainable in the TI. The Δt location corresponded to the location of tumour detected on maxillofacial CT. The temperature difference between lesion and normal zones was of 0.4 °C or higher. Of note, when the tumour was large, then thermal asymmetry in the corresponding TI was easily detected, and image segmentation was not necessary but optional for finding the lesion zone. However, if the tumour was small in size and/or deeply located, then a segmentation of the selected ROI was required for accurate detection of asymmetrical temperature distribution.

As in the case presented in Figure 4, despite CT images showing obvious bone destruction zone, the IRT image can show only slight Δt_{mean} and no clear asymmetry in the TI. Without additional segmentation such small temperature distribution would be undetectable. Image segmentation was helpful or required when the tumour was deeply localized in the oropharyngeal region (Figure 5). In this case, without image segmentation the Δt_{mean} was only of ~0.1 °C and hardly visible, possibly, because of marginal changes of distance from the IRT camera to the patient face. However, after the segmentation of the mouth ROI, the TI appeared asymmetrical the location coincided with the zone revealed during CT evaluation. Quantitative evaluation of segmented mouth ROIs revealed significantly higher values of the Δt_{mean} (0.66 ± 0.1 °C *vs* 0.05 ± 0.19 °C) and Δt_{max} (0.74 ± 0.1 °C *vs* 0.03 ± 0.25 °C) for patients with maxillofacial tumour *vs* the healthy subjects, respectively. This possibly suggests that image segmentation of the ROI of mouth is of particular importance in searching for thermal asymmetry in tumour affected zones, which might be overlooked without such procedures.

In our study, as presented in Figure 6, the Δt values of facial/mouth temperature detected in the healthy volunteers were much smaller in comparison with those of the patients with tumours. Nevertheless, they were variable as well. It is important to note that there was no thermal asymmetry in the TIs of the healthy volunteers even after segmentation of the selected ROI. In a study by others, where young males (age range 18–30 years) without any health problems were investigated, it has been documented that facial Δt values might be variable even in quite homogeneous group.[15]

Variable Δt values could be explained the fact that each group in our study were mixed and included subjects with a different gender, age, ethnicity, and socioeconomic status. In the current study the impact of these factors was not evaluated, but it is known that they have marked impact on the TI data. It is documented that orofacial cancer most often arise in older subjects and in users of tobacco and alcohol, with poor diet and lower socioeconomic status,[16] who usually are irregular dental patients. However, in this study we do not provide a comparison of such data.

On the other hand, physiological factors such as local blood flow, sweating etc. are almost uncontrolled factors that might change the Δt values. Besides, a 15 min equilibration time at the room temperature might be not sufficient after exposure to severe cold, we cannot exclude that Δt values calculated for some patients were influenced of the environmental temperature, since part of IRT data were collected in cold season.

Undoubtedly, many factors could influence the distribution of data obtained from the thermal images of both groups (healthy volunteers or patients with tumours) but this does not change the essence of the IRT diagnostic efficiency, *i.e*. capability to detect Δt asymmetry in the zone of lesion. Maxillofacial cancerous lesions generate more heat, possibly because of an increased blood supply, compared to the surrounding healthy tissue. These differences, as shown in the current study, can be detected by IRT, when using an image processing algorithm with optimized ROI and image segmentation. In addition, our data indicate that in patients with tumours, thermal information obtained after image segmentation of the ROI of mouth cavity is more informative, when compared with the corresponding Δt calculated from the facial skin (Figure 6, g–h *vs* Figure 6 e-f). These data possibly indicate that tumour in facial area should provide heat for larger volume of tissues in order to be visible in the TI, in contrast to the mouth, formed mostly of the mucous membrane.

In the IRT literature,[17,18] it has been proposed that in malignant conditions there were no temperature changes seen until the tumours were large enough to cause necrosis, and this resulted in associated cold spots. However, at present, no detailed analysis has been presented about the rise of temperature depending on tumour stage and/or size. Note that in cases presented here no necrosis zones were obtained in CT images, but we managed to detect clearly the zones of asymmetrical temperature in the TI, when segmentation for the selected ROI was applied. This is in accordance with the opinion that infrared imaging gives a reflection on metabolic activity that allows for detection of tumour induced angiogenesis leading to the development of vascularization much before any other changes appeared.

Summarizing, the detailed comparison of TIs and CT images obtained from the same patient, IRT revealed the presence of temperature asymmetry as well as its location side (*i.e.* coincide with CT results) in all cases. However, image segmentation should be used for accurate unravelling of the affected zones, especially when the tumour is small or deeply located. Importantly, previous studies stated that the average temperature difference between separate anatomical regions should be about 0.4 °C,[3,11] in order to confirm the presence of pathology. The results of the current study suggest that such criterion may not always be valid. We showed that even very small the temperature asymmetry (~0.1 °C) in the TI could be detected with IRT, but image segmentation was needed for this.

Limitations

The segmentation of TIs enables us to highlight a local higher temperature zone from the rest of the face/mouth. Despite our algorithm for automatic processing of thermal images the investigator should check the computer-generated diagnosis, which is based on the detection of zones with asymmetrical temperature. To be able visualizing tumours at their early growth stages, accurate calculations must be done. For this, application of artificial intelligence algorithm should be applied, and this will be explored in our future work.

Conclusions

The results of this study show that the presence of asymmetrical temperature zones and their location, as detected from thermal images, coincide well with the presence and localization of maxillofacial pathologies established by CT. However, accurate information could be obtained only after application of image segmentation algorithm to the selected ROI. Our study demonstrates that image segmentation could help in identifying affected zones when pathology is small or deeply located, and not seen from the TI.

Clinical relevance:
Contemporary gold-standard methods for maxillofacial cancer detection and confirmation are CT scanning and biopsy report. Unfortunately, both of them are not safe. More importantly, they are most efficient for the diagnosis of late stages of the maxillofacial lesions, *i.e*. when the anatomical changes are present. Therefore, cancer detection, especially in its early stage, could benefit from the use of thermal images.

- In our study, the applicability of IRT (a physiological test) for the detection of maxillofacial lesion is based on the correlation with results obtained using CT evaluation (an anatomical test), and confirmation with a histologically proven diagnosis of tumour. Cancerous maxillofacial lesions generate more heat, possibly, because of an increased blood supply, compared to the surrounding healthy skin, and these Δt

differences can be measured by IRT.
- A new IRT algorithm, that optimizes the chosen region (ROI), allows detecting the exact place where the asymmetrical temperature in the maxillofacial region originates. TI data validation by CT and histopathology is an important step toward the clinical application of IRT for the evaluation of maxillofacial lesions.
- In the study, both techniques (CT and IRT) yielded the same results for revealing the presence (or not) of a tumour lesion and its anatomical localization. Nevertheless IRT is not a replacement for CT. IRT, due to its non-invasiveness, may be used during clinical evaluation of patient as an additional screening tool in searching the lesions and continuation of its progression in the maxillofacial region. For this, artificial intelligence algorithm with an automatic recognition of lesions must be used.

References

1. Ring EF, Ammer K. Infrared thermal imaging in medicine. *Physiol Meas* 2012; **33**: R33–R46. doi: https://doi.org/10.1088/0967-3334/33/3/R33
2. Lahiri BB, Bagavathiappan S, Jayakumar T, Philip J. Medical applications of infrared thermography: a review. *Infrared Phys Technol* 2012; **55**: 221–35. doi: https://doi.org/10.1016/j.infrared.2012.03.007
3. Gratt BM, Graff-Radford SB, Shetty V, Solberg WK, Sickles EA. A 6-year clinical assessment of electronic facial thermography. *Dentomaxillofac Radiol* 1996; **25**: 247–55. doi: https://doi.org/10.1259/dmfr.25.5.9161178
4. Duarte A, Carrão L, Espanha M, Viana T, Freitas D, Bártolo P, et al. Segmentation algorithms for thermal images. *Procedia Technology* 2014; **16**: 1560–9. doi: https://doi.org/10.1016/j.protcy.2014.10.178
5. Ring EFJ, Ammer K. The technique of infra red imaging in medicine. *Thermol Int* 2000; **10**: 7–14.
6. Acharya UR, Ng EYK, Sree SV, Chua CK, Chattopadhyay S, EYK N. Higher order spectra analysis of breast thermograms for the automated identification of breast cancer. *Expert Systems* 2014; **31**: 37–47. doi: https://doi.org/10.1111/j.1468-0394.2012.00654.x
7. Shrivakshan GT. A comparison of various edge detection techniques used in image processing. *IJCSI International Journal of Computer Science* 2012; **9**(Iss5, No1): 272–6.
8. Prewitt JMS. Object enhancement and extraction. In: Lipkin B, Rosenfeld A, eds. *Picture processing and Psychopictorics*. New York: Academic Press; 1970. pp. 75–149.
9. Barber CB, Dobkin DP, Huhdanpaa H. The quickhull algorithm for convex hulls. *ACM Transactions on Mathematical Software* 1996; **22**: 469–83. doi: https://doi.org/10.1145/235815.235821
10. Mostovoy A. Thermography and oral pathology. *EAT2012 Book of Proceedings – Appendix 1 of Thermology international* 2012; **22**: 159–61.
11. Durnovo EA, Potekhina YUP, Marochkina MS, Khomutinnikova NE, Yanova NA. Features of infrared thermography in the diagnosis of complex diseases of maxillofacial region. *Modern Problems of Science and Education* 2012.
12. Christensen J, Vaeth M, Wenzel A. Thermographic imaging of facial skin--gender differences and temperature changes over time in healthy subjects. *Dentomaxillofac Radiol* 2012; **41**: 662–7. doi: https://doi.org/10.1259/dmfr/55922484
13. Christensen J, Matzen LH, Vaeth M, Schou S, Wenzel A. Thermography as a quantitative imaging method for assessing postoperative inflammation. *Dentomaxillofac Radiol* 2012; **41**: 494–9. doi: https://doi.org/10.1259/dmfr/98447974
14. Rodrigues-Bigaton D, Dibai-Filho AV, Packer AC, Costa AC, de Castro EM. Accuracy of two forms of infrared image analysis of the masticatory muscles in the diagnosis of myogenous temporomandibular disorder. *J Bodyw Mov Ther* 2014; **18**: 49–55. doi: https://doi.org/10.1016/j.jbmt.2013.05.005
15. Zaproudina N, Varmavuo V, Airaksinen O, Närhi M. Reproducibility of infrared thermography measurements in healthy individuals. *Physiol Meas* 2008; **29**: 515–24. doi: https://doi.org/10.1088/0967-3334/29/4/007
16. Conway DI, Petticrew M, Marlborough H, Berthiller J, Hashibe M, Macpherson LM. Socioeconomic inequalities and oral cancer risk: a systematic review and meta-analysis of case-control studies. *Int J Cancer* 2008; **122**: 2811–9. doi: https://doi.org/10.1002/ijc.23430
17. Hayase Y, Wakasa T, Uemura M, Adachi K, Ochi S, Kishi K. Clinical evaluation of thermography in the diagnosis of malignant tumors in the oral and maxillo-facial region. *Oral Radiol.* 1992; **8**: 11–17. doi: https://doi.org/10.1007/BF02347273
18. Pogrel MA, Yen C-K, Taylor RC. Infrared thermography in oral and maxillofacial surgery. *Oral Surgery, Oral Medicine, Oral Pathology* 1989; **67**: 126–31. doi: https://doi.org/10.1016/0030-4220(89)90315-0